Molecular Crystals and Liquid Crystals

ISSN: 1542-1406 (Print) 1563-5287 (Online) Journal homepage: http://www.tandfonline.com/loi/gmcl20

Biohybrids Based on Carbon Nanotubes and Liposomes – Biophysical Studies

M. E. Barbinta Patrascu, C. Ungureanu & I. Rau

To cite this article: M. E. Barbinta Patrascu, C. Ungureanu & I. Rau (2014) Biohybrids Based on Carbon Nanotubes and Liposomes – Biophysical Studies, Molecular Crystals and Liquid Crystals, 604:1, 1-10, DOI: 10.1080/15421406.2014.978553

To link to this article: http://dx.doi.org/10.1080/15421406.2014.978553

Published online: 15 Dec 2014.

Mol. Cryst. Liq. Cryst., Vol. 604: pp. 1–10, 2014

ISSN: 1542-1406 print/1563-5287 online
DOI: 10.1080/15421406.2014.978553

Taylor & Francis
Taylor & Francis Group

Biohybrids Based on Carbon Nanotubes and Liposomes – Biophysical Studies

M. E. BARBINTA PATRASCU,[1] C. UNGUREANU,[2,*] AND I. RAU[2]

[1]University of Bucharest, Faculty of Physics, Magurele, Romania
[2]University POLITEHNICA of Bucharest, Faculty of Applied Chemistry and Materials Science, Bucharest, Romania

This paper presents a simple and effective bottom-up approach to design novel biohybrids based on biomimetic membranes and carbon nanotubes. Multilamellar and unilamellar lipid vesicles loaded with two antioxidants (quercetin and chlorophyll a*) were obtained by thin film hydration method and have been used to prepare two types of biohybrid systems by addition of carbon nanotubes to these liposome suspensions. Chlorophyll* a *inserted into biomimetic membranes was used as a spectral marker to detect the changes occurred in the artificial lipid bilayers. The obtained carbon-based biohybrids exhibited antioxidant and antimicrobial properties and also a good physical stability.*

Keywords liposomes; chlorophyll; quercetin; carbon nanotubes; antioxidant and antimicrobial activity; biohybrids

1. Introduction

In the last decade, carbon-based nanotechnology gained a significant impact in the biomedical and biotechnological fields [1–3].

Carbon nanotubes (CNTs) are carbon allotropes consisting of graphene sheets rolled up into cylindrical tubes with nanometric diameters and few micrometers in length which serve as building blocks to construct nanohybrids. Depending on number of graphene layers, CNTs are divided into two main classes: single-walled CNTs (SWCNTs) and multiwalled CNTs (MWCNTs). Since their discovery by Iijima in 1991 [4], CNTs have played a key role in nanotechnology due to their unusual properties being considered attractive building blocks to construct improved composite materials. The properties of CNTs could be enhanced by their functionalization leading to hybrid materials with interesting features. In the last years, new approaches in the design of novel composite materials based on carbon nanotubes have been reported [5–6].

In this study, a bottom-up design strategy was employed to obtain biohybrids by noncovalent functionalization of carbon nanotubes with biomimetic phospholipidic membranes

*Address correspondence to Camelia Ungureanu, General Chemistry Department, Faculty of Applied Chemistry and Materials Science, University Politehnica of Bucharest, Romania, 1-7 Polizu, 011061 Bucharest, Romania. E-mail: c_ungureanu@chim.pub.ro; ungureanucamelia@gmail.com

Color versions of one or more of the figures in the article can be found online at www.tandfonline.com/gmcl.

(termed *liposomes*). The functionalization of carbon nanotubes with lipid model membranes was recently reported [7–9] having the advantage to be rapid, non-destructive and confers biocompatibility of carbon nanotubes, making the phospholipids a very attractive soft material largely used in nanotechnology [10].

Liposomes are nanosized vesicles consisting of one or more lipid bilayers (lipophilic compartments) called *lamellae* separated by aqueous layers (hydrophilic compartments); the structure of these artificial lipid bilayers is similar with that of natural membranes and for this reason liposomes are considered analogues of biomembranes. Liposomes are largely used in many areas of nanotechnology especially in biomedical applications as drug delivery systems or as sensing platforms. The lipid based delivery systems are recognized to be low-cost and efficient to carry various active components [10–13].

In this study, liposomes were loaded with two phytochemicals: chlorophyll *a* (Chl*a*) and quercetin, which are recognized as antioxidants acting to retard/prevent the oxidative damage of lipid vesicles [14–16]. Quercetin (*3,3′,4′,5,7-pentahydroxyflavone*) is a flavonol-type flavonoid widely encountered amongst plants (e.g.: onions, apples, red wine, tea, berries etc.), one of the most effective antioxidant due to its chemical structure supporting the scavenging of free radicals. Liposomal quercetin is known to decrease the hepatotoxic effect of carbon tetrachloride and also possesses enhanced antitumor activity and pronounced antioxidant effect [16].

Different biophysical methods were used to characterize the obtained biohybrid systems: UV-VIS absorption and fluorescence emission spectroscopy, zeta potential and Dynamic Light Scattering (DLS) measurements. The *in vitro* antioxidant properties of the bioconstructs were evaluated by chemiluminescence (CL) technique. The agar diffusion method was employed to assess the antibacterial activity of the samples against the microorganism *Escherichia coli.*

Due to its spectral features (strong visible absorption and fluorescence emission), Chl*a* was used as a spectral sensor for the interactions at molecular level occurring in the artificial lipid bilayers.

2. Materials and Methods

2.1. Materials

KH_2PO_4, Na_2HPO_4, luminol (5-amino-2,3-dihydro-phthalazine-1,4-dione), Tris (hydroxymethylaminomethane base), HCl, H_2O_2 were purchased from Merck (Germany). Chloroform, 70% ethanol, SWCNTs, dipalmitoyl phosphatidylcholine (DPPC), Quercetin (Q) and cholesterol (Chol) were supplied from Sigma Aldrich (Germany).

The antibacterial activity was tested against human pathogenic microbial strain *Escherichia coli* ATCC 8738. The bacterial strains were grown in Luria Bertani Agar (LBA) plates at 37°C with following composition: peptone (Merck) 10 g/L; yeast extract (Biolife) 5 g/L, NaCl (Sigma-Aldrich) 5 g/L and agar (Fluka) 20 g/L.

2.2. Preparation of Liposomes

Multilamellar lipid vesicles (MLVs) were obtained by thin film hydration method [17], using DPPC and cholesterol (Chol) as lipids (Chol/DPPC molar ratio = 1/4). The lipid vesicles were suspended in a phosphate buffer solution (PB): KH_2PO_4–Na_2HPO_4 pH 7.4.

Table 1. The codes of the prepared samples

Sample	Code
Chl*a*-Chol-DPPC-Q-MLVs	A
Chl*a*-Chol-DPPC-Q-SUVs	B
Chl*a*-Chol-DPPC-Q-MLVs/SWCNTs	C
Chl*a*-Chol-DPPC-Q-SUVs/SWCNTs	D

Cholesterol was introduced in the artificial lipid bilayers in order to improve the physical stability of the lipid vesicles [18, 19].

Chlorophyll *a* extracted from fresh spinach leaves as described previously [20] was incorporated into artificial lipid bilayers (Chl*a*/lipid molar ratio = 1/100) during the lipid film preparation, in order to use this phytopigment as a spectral marker, to monitor the modifications occurred in the biomimetic membranes. Our previous work [21–26] demonstrated that Chl*a* is an excellent sensor to detect any change happened in artificial lipid bilayers. Quercetin (Q), a plant pigment and a powerful natural antioxidant, was inserted in lipid membranes (Q/lipid molar ratio = 1/100). Small unilamellar lipid vesicles (SUVs) were prepared from MLV suspensions by exposure to ultrasounds using a titanium probe sonicator (15 min, Hielser, UP 100 H).

These procedures were performed above the critical temperature (T_c) of phase transition of lipids resulting in liquid crystalline lipid membranes.

2.3. Preparation of Liposomes/SWCNTs Biohybrids

Single walled carbon nanotubes (SWCNTs) have been added to suspensions of MLVs and SUVs, in the ratio SWCNT/liposome suspension = 0.05 mg/mL. Each mixed suspension was further subjected to ultrasound treatment using the above mentioned titanium probe sonicator, resulting in MLVs/SWCNTs and SUVs/SWCNTs biohybrid formation. In Table 1 are presented the prepared samples.

All the experiments were carried out in dark to avoid photodegradation of the samples.

2.4. Characterization Methods

The absorption spectra of liposomes and carbon-based biohybrids were recorded on a double beam spectrophotometer Lambda 2S Perkin Elmer, in 200–800 nm wavelength range, operated at a resolution of 1 nm.

The fluorescence emission spectra of Chl*a* in liposomes and biocomposites were performed on a LS55 PERKIN-ELMER spectrophotofluorimeter, by illuminating the samples with a 430 nm excitation light and the fluorescence emission was collected at 630–750 nm.

The hydrodynamic diameters, $Z_{average}$ (the particle diameter plus the double layer thickness) of the samples were measured by DLS technique (Zetasizer Nano ZS, Malvern Instruments Ltd., U.K.), at 25°C temperature and at a scattering angle of 90°. The intensity distribution was used to evaluate the particle size analysis data. For each sample, the mean diameter and the polydispersity index (PdI) were calculated from three individual measurements and the mean values (±standard deviation, SD) were further reported.

The zeta potential (ZP) values of the lipid vesicles and of the biohybrids were measured using an appropriate dispositive of Zetasizer Nano ZS (Malvern Instruments Ltd., U.K.)

by applying an electric field across the analyzed aqueous dispersions. These measurements were performed in triplicate and the mean values (±SD) were reported.

The *in vitro* antioxidant activity of the samples has been determined by chemiluminescence (CL) method on a Chemiluminometer Turner Design TD 20/20, USA, using luminol + H_2O_2 in alkaline buffer (pH = 8.6) as a generator of free radicals of oxygen. The antioxidant activity (AA%), as percentage of free radical scavenging was calculated from the relation:

$$AA = [(I_0 - I)/I_0] \cdot 100\% \quad (1)$$

where I_0 is the maximum CL intensity for standard at t = 5 s and I is the maximum CL intensity for sample at t = 5 s [12].

The antimicrobial activities of liposomes and biocomposites were investigated under aseptic conditions, using the Disk Diffusion method against pathogenic microorganism *Escherichia coli* ATCC 8738 (Gram (-) bacterium). The control experiment consists of a plate of solidified agar onto which was inoculated 50 μL of pure solvent (PB) as reported by Murray et al. [27]. The aseptic chamber consisting of a wooden box with a door was cleaned with 70% ethanol and irradiated with short wave UV light for 1 hour. Sterile plates were prepared by pouring the sterilized media in sterile Petri dishes under aseptic conditions. The test organism (1 mL) was spread on agar plates. Using a sterile Durham tube of 6 mm diameter, the wells were made according to the number of samples. The wells were inoculated with 50 μL of each sample. Antibacterial activity of the samples was determined by measuring the size of inhibition zone (IZ, mm) as a clear, distinct zones of inhibition surrounding agar wells, and values less than 8 mm were considered as not active against microorganism. All of the experiments were performed in triplicate; the results reported as the average of three experiments are presented as mean ± SD.

3. Results and Discussion

3.1. Characterization of Chla-Liposomes and Biohybrids by Visible Absorption Spectroscopy

Figure 1 displayed the absorption spectra of all the samples. Chl*a* embedded in artificial lipid bilayers was used as a spectral marker and some spectral criteria were developed to monitor the interactions between CNTs and liposomes. All spectra were corrected as regarding the Rayleigh scattering as described previously [21, 22, 25] and then normalized *versus* the absorption at the maximum in red.

The addition of SWCNTs to liposome suspensions has no effect on the position of the Chl*a* red maximum (671 nm for samples A and C; 670 nm for B and D), so the location of Chl*a* in lipid bilayers was not affected, the porphyrin ring of Chl*a* maintaining its location at the lipid-water interface in the vicinity of polar lipid heads [21].

The presence of the carbon nanotubes affected the dimensions of the lipid vesicles highlighted by a decrease in the Soret band absorbance ratios (by 3.27% for MLVs and by 3.13% for SUVs). The interaction liposomes/carbon nanotubes probably resulted in structural reorganization of liposomal membranes.

Carbon-based biohybrids are larger in size, so the position of the spectrum baseline is higher for these samples (C and D) as compared to that of liposomes.

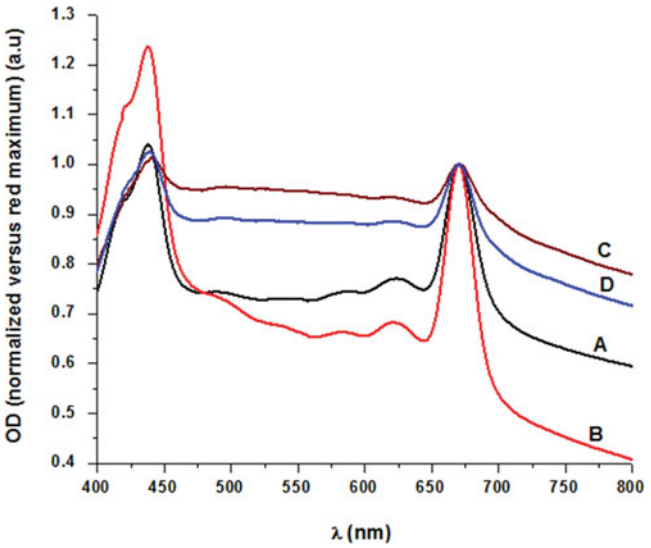

Figure 1. The VIS absorption spectra of Chl*a* in liposomes and in liposomes/SWCNTs biocomposites.

3.2. The Fluorescence Emission Spectra of Chla in Liposomes and Biocomposites

Figure 2 shows the emission spectra of Chl*a* embedded in liposomes as a fluorescence probe, using excitation wavelength of 430 nm. The fluorophore - the porphyrin macrocycle of Chl*a* is located at the lipid-water interface in the vicinity of polar lipid heads, and the phytyl tail in the hydrophobic lipid chains region [28].

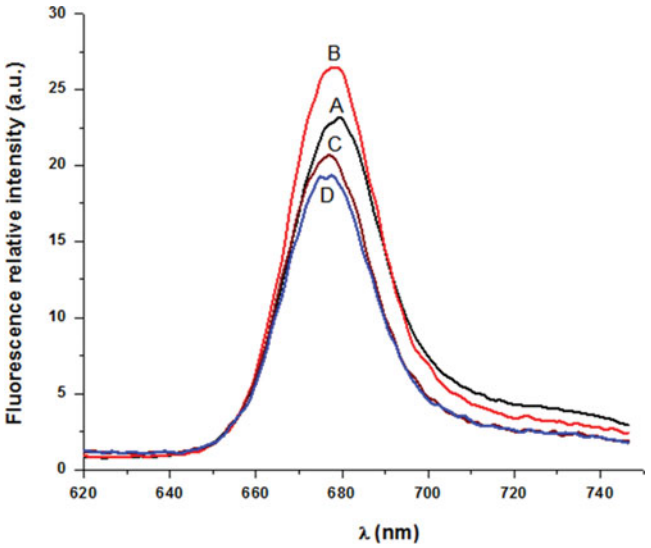

Figure 2. Fluorescence emission spectra of Chl*a* in liposomes and in biocomposites liposomes/SWCNTs (the excitation wavelength was 430 nm).

Table 2. DLS data and zeta potential values of the samples

Sample	Zeta Potential [mV]	$Z_{average}$[nm]	PdI
A	-16.3 ± 0.95	573 ± 7.9	0.327 ± 0.031
B	-26.1 ± 2.5	139.2 ± 1.097	0.331 ± 0.014
C	-41.8 ± 1.14	656.4 ± 39.67	0.333 ± 0.077
D	-39.9 ± 2.65	352.2 ± 11.87	0.387 ± 0.031

The emission peak of Chl*a* incorporated in MLVs is blue shifted from 679.5 nm to 677 nm in MLVs/CNTs biohybrids as compared to the main fluorimetric peak of Chl*a* embedded in SUVs which is blue shifted from 678.5 nm to 677.5 nm in SUVs/CNTs composites, indicating that Chl*a* sensed a less polar environment. The shift was more pronounced in the case of MLVs.

The fluorescence quenching in the case of MLVs towards SUVs could be explained by an efficient energy transfer between chlorophyll molecules of MLV lamella. The emission spectra of Chl*a* revealed also a fluorescence quenching in the case of nanobiocomposites, probably due to the efficientization of energy transfer between the Chl*a* molecules embedded in the lipid bilayers of the biomimetic membranes deposed along the carbon nanotube surfaces.

3.3. Particle Size and Zeta Potential of the Liposomes and CNTs/Liposomes Biocomposites

DLS analysis is widely used to monitor the particle size from various dispersions. The physical stability of the samples was evaluated in terms of zeta potential (ZP). The DLS results and zeta potential values of the samples are showed in Table 2.

The particle size analysis of MLVs revealed high value of average diameter (573 nm) and short-term stability (ZP = −16.3 mV). After the sonication process, the size of MLVs strongly decreased resulting in small unilamellar vesicles with a mean diameter of 139.2 nm

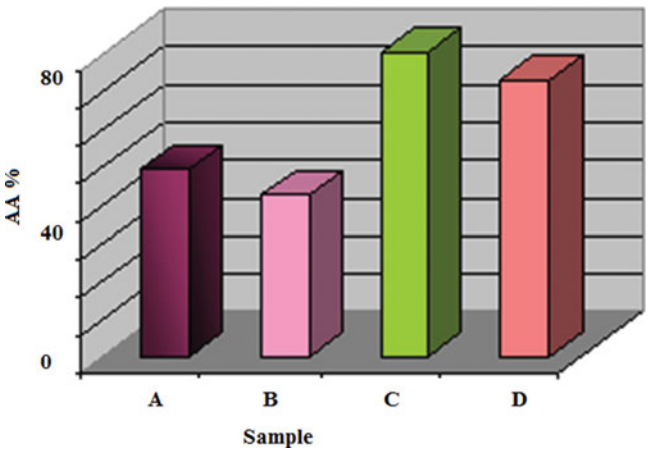

Figure 3. Antioxidant properties of the samples.

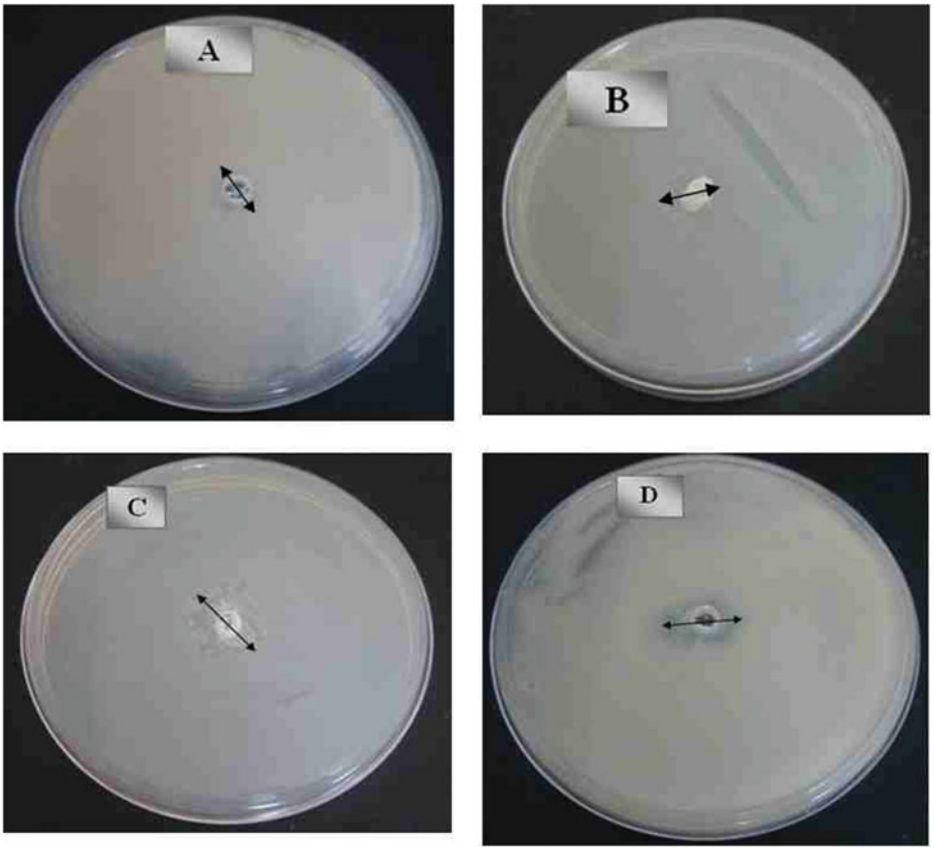

Figure 4. Comparative antibacterial activity of samples against *E. coli*.

and a good polydispersity index (0.331) which presented a moderate stability in time (ZP = −26.1 mV).

The carbon-based biohybrids exhibited larger size than liposomes alone and also a higher stability, the most stable being the Chl*a*-Chol-DPPC-Q-MLVs/SWCNTs (see sample C) biocomposites (ZP = −41.8 mV).

3.4. Evaluation of Antioxidant Properties of the Samples

As it can be seen from Fig. 3, all the samples exhibited antioxidant properties. The antioxidant behaviour of the liposomes was due to the presence of chlorophyll (1%) and quercetin (1%) in the artificial lipid membranes. These phytocompounds are recognized to possess antioxidative potential [14–16].

The presence of CNTs enhances by 64.17% the antioxidant activity of MLVs which reached the value of 80.1% in MLVs/SWCNTs hybrids. In the case of unilamellar liposomes, it was observed an AA enhancement by 71.48% in the SUVs/SWCNTs biocomposites (AA = 72.9%).

The Chl*a*-Chol-DPPC-Q-MLVs/SWCNTs biohybrid (see sample C) proved to be the most effective against oxidative attack of free radicals generated in the alkaline system containing luminol (see section 2.4).

Table 3. Antimicrobial activities (measured as *diameter*, in mm and *area*, in mm^2 of inhibition zone) of the samples, against *Escherichia coli* ATCC 8738

Sample	Mean diameter ± SD (mm)	Area of inhibition zone (mm^2)
A	10 ± 0.057	78.50
B	11 ± 0.12	94.98
C	19 ± 0.08	283.38
D	17 ± 0.1	226.86

3.5. Antimicrobial Activity of Liposomes and CNTs/Liposomes Biohybrids

The antimicrobial investigations were performed on Gram-negative bacterium *Escherichia coli* ATCC 8738 using the phosphate buffer solution pH 7.4 as a negative control.

The comparative results of antibacterial investigations of samples against *E. coli* are comparatively presented in Fig. 4. The agar plate images showed that sample C was the most efficient against *E. coli* exhibiting the highest area of inhibition zone.

Both types of biomimetic membranes (A and B) exhibited antibacterial activity due to their content of chlorophyll and quercetin phyto-molecules recognized to possess antimicrobial properties [29–33]. On the other hand, the nanometric size of liposomes confers them the opportunity to strongly interact at this scale with the nano-sized components of bacteria cells resulting in perturbation of the microbial lipid membranes and finally their disruption.

No significant difference it was observed regarding the antimicrobial activity of MLVs (sample A) compared to SUVs (sample A) showing inhibition zone of 10 mm and 11 mm, respectively. When the carbon nanotubes are present, the inhibition zone diameter enhanced by 90% in the case of MLVs and by 54.5% in the case of SUVs (Table 3). Thus, regarding the area of inhibition zone (see Table 3), the MLVs/SWCNTs biohybrids exhibited the highest value (283.38 mm^2); these hybrids proved to be the most potent against *E.coli*.

4. Conclusion

Noncovalent entities based on carbon nanotubes and antioxidant liposomes were achieved by a bottom-up strategy leading to improved nano-biostructures. Addition of carbon nanotubes to liposomal suspensions resulted in hybrid systems with improved properties.

Chlorophyll *a* proved to be an excellent molecular sensor to get useful information regarding the modifications occurred in the liposomal membranes. The absorption and emission spectral features of Chl*a* inserted in liposomes were changed as a result of interaction between CNTs and artificial lipid bilayers. Chl*a* sensed a structural reorganization of liposomal membranes, more pronounced in the case of multilamellar lipid vesicles.

Between all the samples, MLVs/SWCNTs hybrids presented the best antioxidant (AA = 80.1%) and antimicrobial properties (offering the highest inhibition zone of 19 mm against *E. coli*) and a good physical stability (ZP = −41.8 mV).

Also it was observed a good correlation between the visible absorption and fluorescence emission spectra and DLS results.

Building Chl*a*-flavonoid-loaded biomimetic membranes/SWCNTs biohybrids is promising for biomedical and biotechnological applications as antioxidant and antimicrobial coatings.

References

[1] Gong, H., Peng, R., & Liu, Z. (2013). *Adv. Drug Deliver. Rev.*, *65*(15), 1951.
[2] Iannazzo, D., Piperno, A., Pistone A., Grassi, G., & Galvagno, S. (2013). *Curr. Med. Chem.*, *20*(11), 1333.
[3] Zhang, X., Guo, Q., & Cui, D. (2009). *Sensors*, *9*, 1033.
[4] Iijima, S. (1991). *Nature*, *354*, 56.
[5] Chuekachang, S., Janmanee, R., Baba, A., Phanichphant, S., Sriwichai, S., Shinbo, K., Kato, K., Kaneko, F., Fukuda, N., & Ushijima, H. (2013). *Mol. Cryst. Liq. Cryst.*, *580*(1), 1.
[6] Netsuwan, P., Sriwichai, S., Phanichphant, S., Baba, A., Shinbo, K., Kato, K., & Kaneko, F. (2013). *Mol. Cryst. Liq. Cryst.*, *580*(1), 7.
[7] Barbinta Patrascu, M. E., Cojocariu, A., Tugulea, L., Badea, N. M., Lacatusu, I., & Meghea, A. (2011). *J. Optoelectron. Adv. Mat.*, *13*(9), 1165.
[8] Debouzy, J. C., Crouzier, D., & Flahaut, E. (2010). *Env. Toxicol. Pharmacology*, *30*(2), 147.
[9] Huang, Y., Palkar, P. V., Li, L. J., Zhang, H., & Chen, P. (2010). *Biosens. Bioelectron.*, *25*, 1834.
[10] Mashaghi, S., Jadidi, T., Koenderink, G., & Mashaghi, A. (2013). *Int. J. Mol. Sci.*, *14*, 4242.
[11] Lacatusu, I., Badea, N., Murariu, A., Bojin, D., & Meghea, A. (2010). *Mol. Cryst. Liq. Cryst.*, *523*, 247.
[12] Lacatusu, I., Badea, N., Oprea, O., Bojin, D., & Meghea, A. (2012). *J. Nanopart. Res.*, *14*, 902.
[13] Barbinta Patrascu, M. E., Bunghez, I. R., Iordache, S. M., Badea, N., Fierascu, R. C. & Ion, R. M. (2013). *J. Nanosci. Nanotechno.*, *13*, 2051.
[14] Lanfer-Marquez, U. M., Barros, R. M. C., & Sinnecker, P. (2005). *Food Res. Int.*, *38*, 885.
[15] Dentuto, P. L., Catucci, L., Cosma, P., Fini, P., Agostiano, A., Hackbarth, S., Rancan, F., & Roeder, B. (2007). *Bioelectrochemistry*, *70*, 39.
[16] Suntres, Z. E. (2011). *J. Toxicol.*, Article ID 152474, 16 pages, doi:10.1155/2011/152474.
[17] New, R.R.C. (1990). *Liposomes: A Practical Approach*, IRL Press, Oxford University, U.K.
[18] Yang, S., Zheng, Y., Chen, J., Zhang, Q., Zhao, D., Han, D., & Chen, X. (2013). *Colloids Surf., B 101*, 6.
[19] Phillipot, J. R., & Schuber, F. (1995). *Liposomes as Tools in Basic Research and Industry*, CRC Press, Inc., Boca Raton, Florida.
[20] Strain, H. H., & Svec, W. A. (1966). In: *The Chlorophylls*, Vernon, L. P. & Seely, G. R. (Eds.), Chapter *Extraction, separation, estimation, and isolation of the chlorophylls*, Academic Press, New York, USA, 21.
[21] Milenkovic, S. M., Barbinta-Patrascu, M. E., Baranga, G., Markovic, D. Z., & Tugulea, L. (2013). *Gen. Physiol. Biophys.*, *32*(4), 559.
[22] Barbinta Patrascu, M. E., Tugulea, L, Lacatusu, I., & Meghea, A. (2010). *Mol. Cryst. Liq. Cryst.*, *522*, 148.
[23] Stefanescu, T., Manole, C., Parvu, C., Barbinta Patrascu, M. E., & Tugulea, L. (2010). *Optoelectron. Adv. Mat.- Rapid Commun.*, *4*(1), 33.
[24] Barbinta Patrascu, M. E., Tugulea, L., & Meghea, A. (2009). *Rev. Chim.*, *60*(4), 337.
[25] Barbinta Patrascu, M. E., Tugulea, L., Meghea, A., & Popescu, A. (2008). *Optoelectron. Adv. Mat.- R.apid Commun.*, *2*(2), 113.
[26] Barbinta Patrascu, M. E., Ungureanu, C., Iordache, S. M., Iordache, A. M., Bunghez, I. R., Ghiurea, M., Badea, N., Fierascu, R. C., & Stamatin, I. (2014). *Mat. Sci. Eng. C*, *39*, 177.
[27] Murray, P. R., Baron, E. J., Pfaller, M. A., Tenover, F. C., & Yolke, R. H. (1995). *Manual of Clinical Microbiology*, 6th ed. Mosby Year Book, London, UK.
[28] Tugulea, L., & Paşcanu, S. (1996). *Rom. J. Biophys.*, *6*, 1.
[29] Cushnie, T. P. T., & Lamb, A. J. (2005). *Int. J. Antimicrob. Ag.*, *26*, 343.

[30] Habbal, O., Hasson, S. S., El-Hag, A. H., Al-Mahrooqi, Z., Al-Hashmi, N., Al-Bimani, Z., Al-Balushi, M. S., & Al-Jabri, A. A. (2011). *Asian Pacific Journal of Tropical Biomedicine*, 173.
[31] Jayavanth, P., Kaur, K., & Junainah, A. H. (2011). *Journal of Natural Products*, *4*, 94.
[32] Maekawa, L. E., Lamping, R., Marcacci, S., Maekawa, M. Y., Nassri, M. R. G., & Koga-Ito, C. Y. (2007). *RSBO*, *4*(2), 36.
[33] Mowbray, S. B. A. (1957). *British Medical Journal*, *2*, 268.